

Quantum control using sequences of simple control pulses

S. G. Schirmer* and Andrew D. Greentree†

Quantum Processes Group, The Open University, Milton Keynes, MK7 6AA, United Kingdom

Viswanath Ramakrishna‡

*Center for Engineering Math and the Program in Math Sciences,
EC 35, University of Texas at Dallas, Richardson, Texas 75083*

Herschel Rabitz§

Department of Chemistry, Frick Laboratories, Princeton University, Princeton, NJ 08544

(Dated: May 14, 2001)

Structured decompositions of a desired unitary evolution operator are employed to derive control schemes that achieve certain control objectives for finite-level quantum systems using only sequences of simple control pulses such as square-waves with finite rise and decay times or Gaussian wavepackets. The technique is applied to find control schemes that achieve population transfers for pure-state systems, complete inversions of the ensemble populations for mixed-state systems, create arbitrary superposition states and optimize the ensemble average of observables.

PACS numbers: 03.65.Bz

I. INTRODUCTION

The ability to control quantum systems is an essential prerequisite for many present and potential future applications involving the manipulation of atomic and molecular quantum states [1]. Some of the important applications are quantum state engineering [2], control of chemical reactions [3] and laser cooling of internal molecular degrees of freedom [4, 5]. Quantum control theory may also reveal new ways to solve problems crucial to quantum computing such as initializing quantum registers [6] or building robust quantum memory [7].

Due to the wide range of applications, the immediate aims of quantum control may vary. However, the control objective can usually be classified as one of the following:

1. to steer the system from its initial state to a target state with desired properties,
2. to maximize (or minimize) the expectation value (ensemble average) of a selected observable, or
3. to achieve a certain evolution of the system.

Despite their apparent dissimilarity, these control objectives are closely related. Indeed, (1) can be considered a special case of (2) in which the observable is the projector onto the subspace spanned by the target state and (2) is a special case of (3) where we desire to find an evolution operator that maximizes the expectation value of the selected observable either at a specific target time or

at some time in the future. Thus, one of the central problems of quantum control is to achieve a desired evolution of the system by applying external control fields and the primary challenge is to find control pulses (or sequences of such pulses) that are feasible from a practical point of view and effective in realizing the control objective.

Many of the control strategies for quantum systems that have been proposed to date rely on numerical methods to solve the control or optimization problem [8, 9, 10, 11, 12, 13, 14]. In this paper, we explore an alternative approach to quantum control, which is based on explicit generation of unitary operators using Lie group decompositions [15]. The technique uses the rotating wave approximation (RWA) and employs frequency discrimination or other atomic selection rules to address transitions individually. Although these assumptions seem to preclude the application of the technique to some model systems of interest, e.g., systems with equally spaced or almost equally spaced energy levels, it should nevertheless be applicable to many quantum systems. A significant advantage of the approach we pursue in this paper is the flexibility of the control pulse shapes, which makes it possible to choose control pulses that are reasonably simple to create in the laboratory, such as square-wave pulses with finite rise and decay times or Gaussian wavepackets.

II. MATHEMATICAL FORMULATION OF THE CONTROL PROBLEM

We consider a quantum system with a discrete energy spectrum whose energy levels E_n are assumed to be finite, non-degenerate and ordered in an increasing sequence,

$$E_1 < E_2 < \dots < E_N, \quad (1)$$

*Electronic address: s.g.schirmer@open.ac.uk

†Electronic address: a.d.greentree@open.ac.uk

‡Electronic address: vish@utdallas.edu

§Electronic address: hrabitz@chemvax.princeton.edu

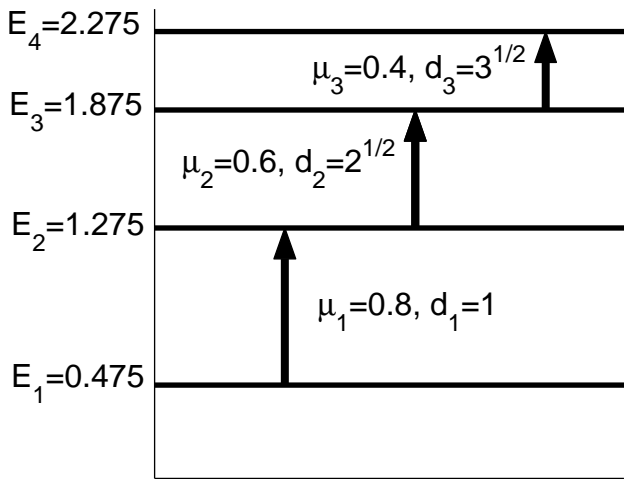


FIG. 1: Energy-level and transition diagram for a four-level Morse oscillator with anharmonicity $\alpha = 0.1$.

where $N < \infty$ is the dimension of the Hilbert space of pure states of the system. Note that non-degeneracy and the particular ordering of the energy levels are assumed primarily for simplicity. These requirements can often be relaxed if selection rules are available to distinguish degenerate energy levels and different transitions that have the same transition frequency. Moreover, non-degeneracy of the energy levels can often be assured by considering suitable subspaces of the Hilbert space of pure states. Our model is strictly valid only for dissipation-free single atoms or optically thin ensembles of homogeneously broadened atoms. However, by choosing appropriately short control times (with respect to the lifetimes of the excited states) [16], our idealized model should be applicable to a variety of quantum systems including many atomic and molecular N -state systems, Rydberg atoms or particles in (anharmonic) quantum wells.

Although the results presented in this paper do not depend on a specific model, for clarity, we shall illustrate our results using a four-level Morse oscillator with energy levels

$$E_n = \hbar\omega_0 \left(n - \frac{1}{2} \right) \left[1 - \alpha \left(n - \frac{1}{2} \right) \right] \quad (2)$$

for $1 \leq n \leq 4$ and transition dipole moments

$$d_n = p_{12}\sqrt{n}, \quad 1 \leq n \leq 3, \quad (3)$$

where ω_0 and p_{12} are constants representing the oscillator frequency and the transition dipole moment of the transition $|1\rangle \rightarrow |2\rangle$, respectively. The parameter α determines the anharmonicity of the system, which we arbitrarily set to 0.1. The energy-level and transition diagram for this system is shown in figure 1.

The free evolution of the system is governed by the

internal Hamiltonian, whose spectral representation is

$$\hat{H}_0 = \sum_{n=1}^N E_n |n\rangle \langle n|, \quad (4)$$

where $\{|n\rangle : n = 1, \dots, N\}$ is a complete set of orthonormal eigenstates that satisfy the stationary Schrödinger equation

$$\hat{H}_0 |n\rangle = E_n |n\rangle, \quad 1 \leq n \leq N. \quad (5)$$

The application of external control fields perturbs the system and gives rise to a new Hamiltonian $\hat{H} = \hat{H}_0 + \hat{H}_I$, where \hat{H}_I is an interaction term. For a control field of the form

$$\begin{aligned} f_m(t) &= 2A_m(t) \cos(\mu_m t + \phi_m) \\ &= A_m(t) \left[e^{i(\mu_m t + \phi_m)} + e^{-i(\mu_m t + \phi_m)} \right], \end{aligned} \quad (6)$$

which is resonant with the transition frequency $\mu_m = E_{m+1} - E_m$ and drives only the transition $|m\rangle \rightarrow |m+1\rangle$, using the rotating wave approximation (RWA) leads to the following interaction term

$$\begin{aligned} \hat{H}_m(f_m) &= A_m(t) e^{i(\mu_m t + \phi_m)} d_m |m\rangle \langle m+1| \\ &\quad + A_m(t) e^{-i(\mu_m t + \phi_m)} d_m |m+1\rangle \langle m|, \end{aligned} \quad (7)$$

where d_m is the transition dipole moment for the transition $|m\rangle \rightarrow |m+1\rangle$, ϕ_m is the initial phase and $2A_m(t)$ is the envelope of the field, which must be slowly varying with respect to μ_m^{-1} . It should be noted that the validity of this approximation for the interaction with the field f_m depends on one's ability to individually address the m th transition, either by use of selection rules or frequency discrimination.

For frequency-selective control the transition frequencies μ_m must be sufficiently distinct to assure that each field is resonant only with a single transition and that off-resonant effects on other transitions are small. To satisfy this requirement, we note that if a monochromatic field of constant amplitude $2A_m$ and frequency μ_m is applied then off-resonant effects can generally be neglected if the Rabi frequency

$$\Omega_m \equiv 2A_m d_m \quad (8)$$

is considerably less than the detuning of the field from off-resonant transitions. Although the situation is somewhat more complicated for fields with varying amplitude, off-resonant effects should remain small as long as

$$\max_t [2A_m(t) d_m] \ll \mu_m - \mu_n, \quad \forall n \neq m, \quad (9)$$

i.e., as long as the peak amplitude $2A_m$ of the control field f_m is sufficiently small. Since the detuning of adjacent transitions for a Morse oscillator with anharmonicity α is $\mu_m - \mu_{m+1} = 2\alpha$, the peak amplitudes of control pulses should be chosen such that

$$A_m \ll \alpha/d_m. \quad (10)$$

The evolution of the controlled system is determined by a time-evolution operator $\hat{U}(t)$, which satisfies the Schrödinger equation

$$i\frac{d}{dt}\hat{U}(t) = \left\{ \hat{H}_0 + \sum_{m=1}^M \hat{H}_m[f_m(t)] \right\} \hat{U}(t), \quad (11)$$

as well as the initial condition $\hat{U}(0) = \hat{I}$, where \hat{I} is the identity operator. Note that throughout this paper we shall choose units such that $\hbar = 1$. Our aim is to achieve a certain evolution of the system by applying a sequence of simple control pulses. Concretely, we seek to dynamically realize a desired unitary operator \hat{U} at a certain target time T , i.e.,

$$\hat{U} = \hat{U}(T). \quad (12)$$

In some cases, we may not wish to specify a target time in advance, in which case we simply attempt to achieve the control objective at some later time $T > 0$.

III. DETERMINATION OF PULSE SEQUENCE USING LIE GROUP DECOMPOSITIONS

To solve the problem of finding the right sequence of control pulses, we apply the interaction picture decomposition of the time-evolution operator $\hat{U}(t)$,

$$\hat{U}(t) = \hat{U}_0(t)\hat{U}_I(t), \quad (13)$$

where $\hat{U}_0(t)$ is the time-evolution operator of the unperturbed system,

$$\hat{U}_0(t) = \exp(-i\hat{H}_0 t) = \sum_{n=1}^N e^{-iE_n t} |n\rangle\langle n| \quad (14)$$

and $\hat{U}_I(t)$ comprises the interaction with the control fields. Inserting (13) into the Schrödinger equation (11) gives

$$\begin{aligned} i\frac{d}{dt}\hat{U}(t) &= \hat{H}_0\hat{U}_0(t)\hat{U}_I(t) + \hat{U}_0(t)i\frac{d}{dt}\hat{U}_I(t) \\ &\doteq \hat{H}_0\hat{U}(t) + \sum_{m=1}^M \hat{H}_m[f_m(t)]\hat{U}_0(t)\hat{U}_I(t), \end{aligned}$$

which leads to

$$i\frac{d}{dt}\hat{U}_I(t) = \hat{U}_0(t)^\dagger \left\{ \sum_{m=1}^M \hat{H}_m[f_m(t)] \right\} \hat{U}_0(t)\hat{U}_I(t). \quad (15)$$

Inserting equations (14) and (7) into the right hand side of equation (15) leads after some simplification (see appendix A) to

$$\frac{d}{dt}\hat{U}_I(t) = \sum_{m=1}^M A_m(t) d_m (\sin \phi_m \hat{x}_m - \cos \phi_m \hat{y}_m) \hat{U}_I(t) \quad (16)$$

where we define

$$\begin{aligned} \hat{e}_{m,n} &\equiv |m\rangle\langle n| \\ \hat{x}_m &\equiv \hat{e}_{m,m+1} - \hat{e}_{m+1,m} \\ \hat{y}_m &\equiv i(\hat{e}_{m,m+1} + \hat{e}_{m+1,m}). \end{aligned} \quad (17)$$

Hence, if we apply a control pulse

$$\begin{aligned} f_k(t) &= 2A_k(t) \cos(\mu_m t + \phi_k) \\ &= A_k(t) \left[e^{i(\mu_m t + \phi_k)} + e^{-i(\mu_m t + \phi_k)} \right], \end{aligned} \quad (18)$$

which is resonant with the transition frequency μ_m , for a time period $t_{k-1} \leq t \leq t_k$ and no other control fields are applied during this time period then we have

$$\hat{U}_I(t) = \hat{V}_k(t)\hat{U}_I(t_{k-1}), \quad (19)$$

where the operator $\hat{V}_k(t)$ is

$$\hat{V}_k(t) = \exp \left[\int_{t_{k-1}}^t A_k(\tau) d\tau d_m (\sin \phi_k \hat{x}_m - \cos \phi_k \hat{y}_m) \right]. \quad (20)$$

Thus, if we partition the time interval $[0, T]$ into K subintervals $[t_{k-1}, t_k]$ such that $t_0 = 0$ and $t_K = T$ and apply a sequence of fixed-frequency control pulses, each resonant with one transition frequency $\mu_m = \mu_{\sigma(k)}$, such that during each time interval only one control field is applied, then we have

$$\hat{U}(T) = \hat{U}_0(T)\hat{U}_I(T) = e^{-i\hat{H}_0 T} \hat{V}_K \hat{V}_{K-1} \cdots \hat{V}_1, \quad (21)$$

where the factors \hat{V}_k are

$$\hat{V}_k = \exp \left[\int_{t_{k-1}}^{t_k} A_k(\tau) d\tau d_{\sigma(k)} (\sin \phi_k \hat{x}_{\sigma(k)} - \cos \phi_k \hat{y}_{\sigma(k)}) \right], \quad (22)$$

$2A_k(t)$ is the envelope of the k th pulse and σ is a mapping from the index set $\{1, \dots, K\}$ to the control index set $\{1, \dots, M\}$ that determines which of the control fields is active for $t \in [t_{k-1}, t_k]$.

It has been shown in [15] that any unitary operator \hat{U} can be decomposed into a product of operators of the type \hat{V}_k and a phase factor $e^{i\Gamma} = \det \hat{U}$, i.e., there exists a positive real number Γ and real numbers C_k and ϕ_k for $1 \leq k \leq K$ and a mapping σ from the index set $\{1, \dots, K\}$ to the control-sources index set $\{1, \dots, M\}$ such that

$$\hat{U} = e^{i\Gamma} \hat{V}_K \hat{V}_{K-1} \cdots \hat{V}_1, \quad (23)$$

where the factors are

$$\hat{V}_k = \exp [C_k (\sin \phi_k \hat{x}_{\sigma(k)} - \cos \phi_k \hat{y}_{\sigma(k)})]. \quad (24)$$

This decomposition of the target operator into a product of generators of the dynamical Lie group determines the sequence in which the lasers are to be turned on and off. A general algorithm to determine the Lie group decomposition for an arbitrary operator \hat{U} is described in appendix B.

Note that in many cases the target operator \hat{U} is unique only up to phase factors, i.e., two unitary operators \hat{U}_1 and \hat{U}_2 in $U(N)$ are equivalent if there exist values $\theta_n \in [0, 2\pi]$ for $1 \leq n \leq N$ such that

$$\hat{U}_2 = \hat{U}_1 \left(\sum_{n=1}^N e^{i\theta_n} |n\rangle\langle n| \right), \quad (25)$$

where $|n\rangle$ are the energy eigenstates. For instance, if the initial state of the system is an arbitrary ensemble of energy eigenstates

$$\hat{\rho}_0 = \sum_{n=1}^N w_n |n\rangle\langle n|, \quad (26)$$

where w_n is the initial population of state $|n\rangle$ satisfying $0 \leq w_n \leq 1$ and $\sum_{n=1}^N w_n = 1$, then we have

$$\begin{aligned} \hat{U}_2 \hat{\rho}_0 \hat{U}_2^\dagger &= \hat{U}_1 \sum_{n=1}^N |n\rangle e^{i\theta_n} w_n e^{-i\theta_n} \langle n| \hat{U}_1^\dagger \\ &= \hat{U}_1 \sum_{n=1}^N w_n |n\rangle\langle n| \hat{U}_1^\dagger = \hat{U}_1 \hat{\rho}_0 \hat{U}_1^\dagger, \end{aligned} \quad (27)$$

i.e., the phase factors $e^{i\theta_n}$ cancel out. Thus, if the initial state of the system is an ensemble of energy eigenstates, which of course includes trivial ensembles such as pure energy eigenstates, then we only need to find a Lie group decomposition of the target operator \hat{U} modulo phase factors, i.e., it suffices to find matrices \hat{V}_k such that

$$\hat{U} \left(\sum_{n=1}^N e^{i\theta_n} |n\rangle\langle n| \right) = \hat{V}_K \hat{V}_{K-1} \cdots \hat{V}_1. \quad (28)$$

Note that decomposition modulo phase factors, when sufficient, is more efficient since it requires in general up to $2(N-1)$ fewer steps than the general decomposition algorithm. See appendix B for details.

IV. AMPLITUDE AND PULSE LENGTH

Comparing equations (22) and (24) shows that the constants C_k in the decomposition (23) determine the pulse area of the k th pulse:

$$\int_{t_{k-1}}^{t_k} 2A_k(\tau) d\tau = 2 \int_{t_{k-1}}^{t_k} A_k(\tau) d\tau \equiv \frac{2C_k}{d_{\sigma(k)}}. \quad (29)$$

There is considerable flexibility as regards the shape of the control pulses that are used. In this paper we consider two simple types of control functions: square-wave pulses with finite rise and decay times and Gaussian wavepackets. The former type of control pulses is convenient since it is easy to realize them the laboratory. In the optical regime, for instance, a combination of CW lasers and Pockel cells can be used to achieve such pulse shapes.

Gaussian control pulses can be derived from pulse laser systems. In addition, the latter type of control pulses has the distinct advantage of minimal frequency dispersion, which is generally desirable for frequency-selective control.

A. Square-wave pulses

If we apply a field of constant amplitude $2A_k$ for a fixed period of time $\Delta t_k = t_k - t_{k-1}$ then A_k is determined by the pulse area constraint (29)

$$A_k \equiv \frac{C_k}{d_{\sigma(k)} \Delta t_k}. \quad (30)$$

Thus, A_k can be adjusted by changing the pulse length Δt_k , which allows us to account for laboratory constraints on the strengths of the control fields and limit undesirable off-resonant effects by ensuring that

$$A_k \ll \min_n |\mu_{n-1} - \mu_n| / d_{\sigma(k)}. \quad (31)$$

Ideal square-wave pulses are rather simple and convenient pulse shapes. However, in practice it is impossible to reproduce square-wave pulses exactly. Rather, each pulse will have a certain rise and decay time τ_0 , which leads to pulse envelopes of the form depicted in Fig. 2. Mathematically, such pulses can be modeled by choosing the envelope of the pulse of the form

$$\begin{aligned} 2A_k(t) &= A_k \{1 + \text{erf}[4(t - \tau_0/2)/\tau_0]\} \\ &\quad + A_k \{1 + \text{erf}[4(t - \Delta t + \tau_0/2)/\tau_0]\} \end{aligned} \quad (32)$$

where $\text{erf}(x)$ is the error function

$$\text{erf}(x) = \frac{2}{\sqrt{\pi}} \int_0^x e^{-t^2} dt. \quad (33)$$

Although this envelope function may appear quite complicated, it turns out that its pulse area is rather simple to compute. Observing that the area

$$\Pi_1 \equiv A_k \int_0^{\tau_0/2} 1 + \text{erf} \left[\frac{4}{\tau_0} \left(t - \frac{\tau_0}{2} \right) \right] dt$$

is equal to the area

$$\begin{aligned} \Pi_2 &\equiv A_k \int_{\tau_0/2}^{\tau_0} 2 - \left\{ 1 + \text{erf} \left[\frac{4}{\tau_0} \left(t - \frac{\tau_0}{2} \right) \right] \right\} dt \\ &= A_k \int_{\tau_0/2}^{\tau_0} 1 - \text{erf} \left[\frac{4}{\tau_0} \left(t - \frac{\tau_0}{2} \right) \right] dt \\ &= A_k \int_{\tau_0/2}^{\tau_0} 1 + \text{erf} \left[\frac{4}{\tau_0} \left(\frac{\tau_0}{2} - t \right) \right] dt \\ &= -A_k \int_{\tau_0/2}^0 1 + \text{erf} \left\{ \frac{4}{\tau_0} \left[\frac{\tau_0}{2} - (\tau_0 - t) \right] \right\} dt \\ &= A_k \int_0^{\tau_0/2} 1 + \text{erf} \left[\frac{4}{\tau_0} \left(t - \frac{\tau_0}{2} \right) \right] dt \end{aligned}$$

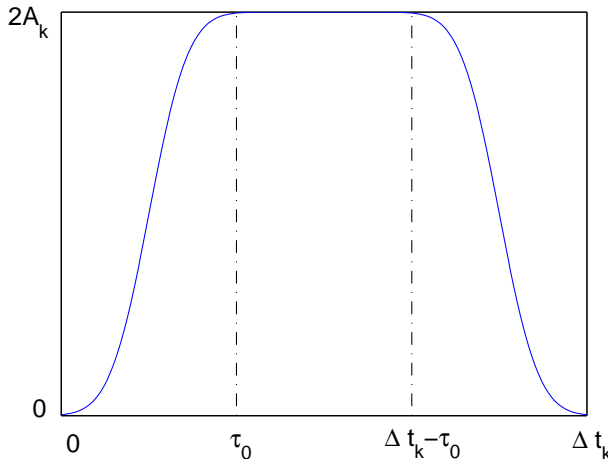


FIG. 2: Square wave pulse of total pulse length Δt_k with rise and decay time τ_0 and peak amplitude $2A_k$

since $-\text{erf}(x) = \text{erf}(-x)$, we note that the total pulse area of a modified square wave pulse of peak amplitude $2A_k$ and total pulse length $\Delta t_k \geq 2\tau_0$ with rise and decay time τ_0 is simply equal to the area of a rectangle of width $\Delta t_k - \tau_0$ and height $2A_k$. Thus, the pulse area constraint (29) leads to $2A_k(\Delta t_k - \tau_0) \equiv 2C_k/d_{\sigma(k)}$ or equivalently

$$A_k \equiv \frac{C_k}{d_{\sigma(k)}(\Delta t_k - \tau_0)}. \quad (34)$$

Although this formula is very similar to (30), note the importance of including the rise and decay time of the pulse. Neglecting τ_0 amounts to overestimating the pulse area, which will result in poor control.

Unless restrictions on the pulse strength dictate otherwise, the pulse lengths Δt_k can be chosen to be the same. For instance, if the target time for achieving the control objective is T and the Lie group decomposition shows that K pulses are required to achieve the control objective, then we would usually set

$$\Delta t_k = \frac{T}{K}, \quad 1 \leq k \leq K. \quad (35)$$

However, recall that it is important to assure that equation (9) is satisfied, i.e., that $2C_k/(\Delta t_k - \tau_0)$ is much smaller than the detuning of the pulse frequency from off-resonant transitions. For instance, for a Morse oscillator with anharmonicity α , the detuning of each pulse from off-resonant transitions is at least 2α and thus $\Delta t_k - \tau_0$ should be much larger than C_k/α in this case.

B. Gaussian wavepackets

If we wish to use Gaussian wavepackets instead of square waves then we choose the envelope of the k th control pulse to be of the form

$$2A_k(t) = 2A_k e^{-q_k^2(t - \Delta t_k/2 - t_{k-1})^2}, \quad (36)$$

which corresponds to a Gaussian wavepacket centered at $t_k^* = t_{k-1} + \Delta t_k/2$ of peak amplitude $2A_k$. The peak amplitude $2A_k$ is determined by the pulse area constraint (29). Concretely, we have

$$A_k \equiv \frac{q_k C_k}{d_{\sigma(k)} \sqrt{\pi}} \quad (37)$$

provided that the k th time interval Δt_k is large enough to justify the assumption

$$\int_{t_{k-1}}^{t_k} e^{-q_k^2(t - \Delta t_k/2 - t_{k-1})^2} dt \approx \int_{-\infty}^{+\infty} e^{-q^2 \tau^2} d\tau = \frac{\sqrt{\pi}}{q_k}.$$

Noting that

$$\int_{-\Delta t_k/2}^{\Delta t_k/2} e^{-q_k^2 t^2} dt = \frac{\sqrt{\pi}}{q_k} \text{erf}(q_k \Delta t_k/2)$$

and $\text{erf}(2) = 0.995322$ we see, for instance, that choosing

$$q_k = \frac{4}{\Delta t_k} \quad (38)$$

guarantees that more than 99% of the pulse area of the k th pulse is contained in the control interval $[t_{k-1}, t_k]$. Choosing $q_k = 6/\Delta t_k$ would ensure that more than 99.99% of the pulse area of the k th pulse is contained in the k th control interval. Again, unless restrictions on the pulse strength dictate otherwise, we set

$$\Delta t_k = \frac{T}{K}, \quad 1 \leq k \leq K, \quad (39)$$

where T is the target time and K is the number of pulses required. Note that the peak amplitude $2A_k$ of the k th field is proportional to q_k , which is in turn inversely proportional to Δt_k . Hence, we can again limit the peak amplitudes and thus off-resonant effects by choosing the pulse lengths Δt_k sufficiently large. In the following sections we apply these results to various control problems.

V. POPULATION TRANSFER $|1\rangle \rightarrow |N\rangle$ FOR A N -LEVEL SYSTEM

Let us first consider a N -level system initially in the ground state $|1\rangle$ and apply the decomposition technique to the simple problem of transferring the population of state $|1\rangle$ to the highest excited state $|N\rangle$ by applying a sequence of monochromatic control pulses, each resonant with one of the transitions frequencies μ_m , which can be regarded as the population inversion route to short-wavelength lasers. It can easily be verified that any evolution operator \hat{U} of the form

$$\hat{U} = \left(\begin{array}{c|c} \mathbf{0} & A_{N-1} \\ \hline e^{i\theta} & \mathbf{0} \end{array} \right), \quad (40)$$

where A_{N-1} is an arbitrary unitary $(N-1) \times (N-1)$ matrix, $e^{i\theta}$ is an arbitrary phase factor and $\mathbf{0}$ is a $N-1$

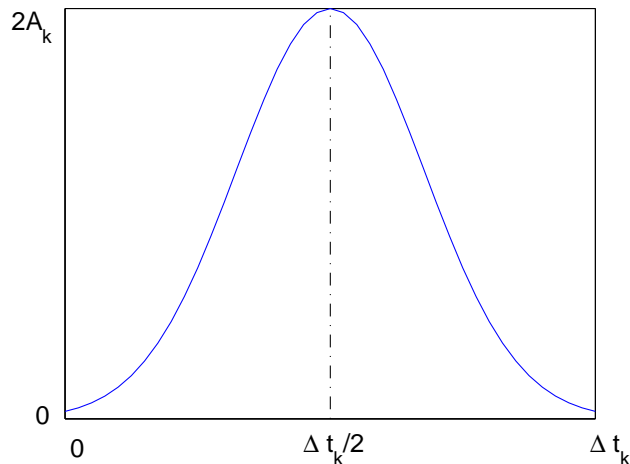


FIG. 3: Gaussian wavepacket with $q_k = \frac{4}{\Delta t_k}$ with peak amplitude $2A_k$

vector whose elements are 0, achieves the control objective since

$$\left(\begin{array}{c|c} \mathbf{0} & A_{N-1} \\ \hline e^{i\theta} & \mathbf{0} \end{array} \right) \begin{pmatrix} 1 \\ \mathbf{0} \end{pmatrix} = \begin{pmatrix} \mathbf{0} \\ e^{i\theta} \end{pmatrix}$$

and thus the population of state $|N\rangle$ is equal to $\sqrt{e^{-i\theta_N} e^{i\theta_N}} = 1$ after application of \hat{U} . Next we observe that setting

$$\hat{U} = \hat{U}_0(T)\hat{U}_I, \quad \hat{U}_I = \hat{V}_{N-1}V_{N-2}\cdots V_1, \quad (41)$$

where the factors are

$$\begin{aligned} \hat{V}_m &= \exp \left[\frac{\pi}{2} (\sin \phi_m \hat{x}_m - \cos \phi_m \hat{y}_m) \right] \\ &= -i(e^{i\phi_m} \hat{e}_{m,m+1} + e^{-i\phi_m} \hat{e}_{m+1,m}) + \sum_{\substack{n \neq m, \\ n \neq m+1}} \hat{e}_{n,n} \end{aligned} \quad (42)$$

for $1 \leq m \leq N-1$, always leads to a \hat{U} of the form (40), independent of the initial pulse phases ϕ_m . This factorization corresponds to a sequence of $N-1$ control pulses, where the m th pulse is resonant with the transition $|m\rangle \rightarrow |m+1\rangle$ and has pulse area π/d_m , which transfers the population step by step to the target level

$$1 \rightarrow 2 \rightarrow 3 \rightarrow \cdots \rightarrow N.$$

Thus, the control sequence derived using the Lie group decomposition technique agrees in this case with the obvious choice of the control pulses.

Figure 4 shows the results of control computations for the four-level Morse oscillator described above using square-wave and Gaussian control pulses, respectively. The top graph in each figure shows the envelopes of the control pulses in units of $10^{-2}\hbar\omega_0/p_{12}$, where ω_0 is the oscillator frequency and p_{12} is the dipole moment of the $1 \rightarrow 2$ transition. The labels f_m for $m = 1, 2, 3$ in the

field plot indicate that the corresponding pulse is resonant with the transition $|m\rangle \rightarrow |m+1\rangle$. The middle graphs shows the evolution of the energy-level populations resulting from the application of the control fields, and the bottom graphs the energy of the system as a function of time, where the upper and lower horizontal lines in the bottom graph indicate the kinematical upper and lower bounds for the energy. Observe that for both choices of the control pulses the final population of target level four is one, i.e., complete population transfer is achieved, while the populations of the intermediate levels increase and decay intermittently.

Also note that the energy of the system increases monotonically from its kinematical minimum value at $t = 0$ to its maximum value at the final time in both cases. The gradient of approach, however, is more uniform for square-wave pulses, while Gaussian pulses tend to result in short, steep increases with long intermittent plateau regions. This is an advantage of using square-wave pulses, which could be significant especially for realistic systems where spontaneous emission is a problem. Gaussian wavepackets on the other hand, have the distinct advantage of minimal frequency dispersion and should thus be less likely to induce unwanted off-resonant effects.

As regards off-resonant effects in general, note that $C_k = \pi/2$ for all pulses. Thus, for our Morse oscillator with $\alpha = 0.1$ and square-wave pulses with rise and decay time $\tau_0 = 30$ time units, we have $C_k/\alpha = 5\pi$, which is much smaller than our choice of $\Delta t_k - \tau_0 = 170$ time units. More precisely, the peak amplitude of field f_m , which is resonant with the transition $|m\rangle \rightarrow |m+1\rangle$, is

$$2A_m = \frac{\pi}{(200-30)\sqrt{m}} \frac{\hbar\omega_0}{p_{12}}.$$

Recalling that the dipole moment is $d_m = \sqrt{m} p_{12}$, the ‘‘Rabi-frequency’’ of the pulse is thus $2A_m d_m / \hbar = \pi/170 \omega_0$, which is less than 1/10 of $0.2 \omega_0$, the detuning of the pulse frequency from closest off-resonant transitions. Note that for fixed pulse lengths, the peak amplitudes for Gaussian control pulses are necessarily larger than for square-wave pulses, in our case by about a factor of 1.5. However, it seems reasonable to assume that Gaussian control pulses that have the same pulse area and pulse length as square-wave pulses should be less likely to cause strong off-resonant effects than square-wave pulses due to smaller frequency dispersion.

VI. INVERSION OF ENSEMBLE POPULATIONS FOR A MIXED-STATE SYSTEM

The results of the previous section are encouraging in that they agree with intuitive control schemes. The power of the decomposition technique, however, lies in its ability to predict control schemes for problems that have no such obvious solutions. One such case is a generalization the control problem discussed in the previous

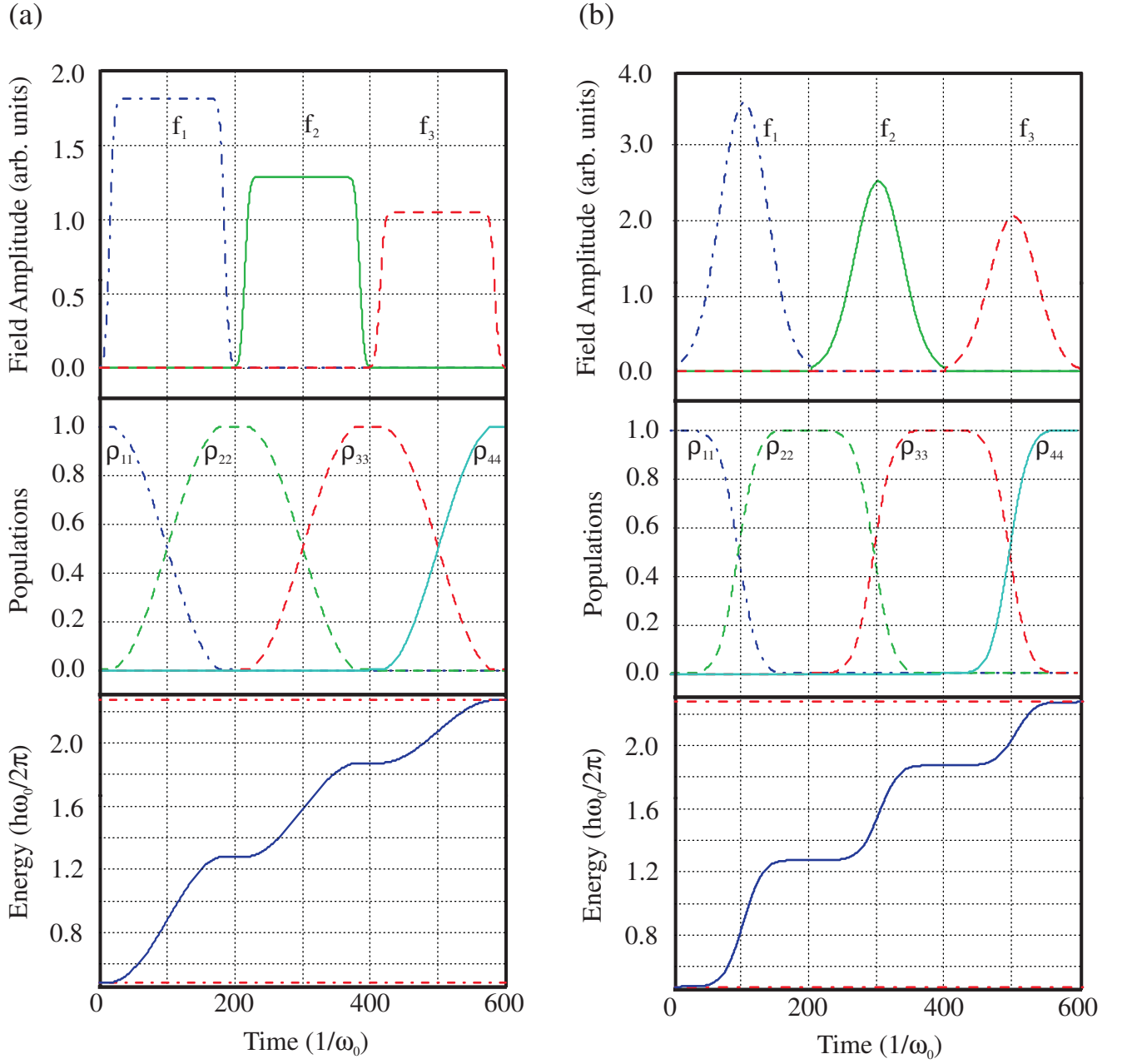


FIG. 4: Population transfer from the ground state $|1\rangle$ to the excited state $|4\rangle$ for the four-level Morse oscillator described above using three square-wave control pulses with rise and decay time $\tau_0 = 30$ time units (a) and Gaussian pulses with shape factor $q = 4/100$ (b). The m th pulse is resonant with the transition $|m\rangle \rightarrow |m+1\rangle$ and has pulse area π/d_m for $m = 1, 2, 3$.

section, where we attempt to achieve complete inversion of the ensemble populations for a N -level system whose initial state $\hat{\rho}_0$ is an arbitrary ensemble of energy eigenstates (26). This control operation can be regarded as a form of generalized NOT gate for mixed-state N -level systems, the ensemble NOT gate, which should not be confused with the U-NOT gate described by Buzek *et al.* in [17].

The desired evolution operator to achieve a complete

reversal of the ensemble populations for the system is

$$\hat{U} = \begin{pmatrix} 0 & 0 & \dots & 0 & e^{i\theta_1} \\ 0 & 0 & \dots & e^{i\theta_2} & 0 \\ \vdots & \vdots & & \vdots & \vdots \\ 0 & e^{i\theta_{N-1}} & \dots & 0 & 0 \\ e^{i\theta_N} & 0 & \dots & 0 & 0 \end{pmatrix}, \quad (43)$$

where the $e^{i\theta_n}$ are arbitrary phase factors. Assuming as above that each transition between adjacent energy

levels can be individually addressed by selecting the frequency of the control pulse and possibly by using other selection rules, the generators of the dynamical Lie algebra are again of the form (22) and a possible Lie group decomposition in terms of these generators is given by

$$\hat{U} = \hat{U}_0(T) \prod_{\ell=N-1}^1 \left[\prod_{m=1}^{\ell} \hat{V}_m \right], \quad (44)$$

where the factors \hat{V}_m are as defined in (42). This decomposition corresponds to a sequence of $K = N(N-1)/2$ control pulses

$$f_1, f_2, \dots, f_{N-1}, f_1, f_2, \dots, f_{N-2}, \dots, f_1, f_2, f_1,$$

where the k th pulse is resonant with the transition $|\sigma(k)\rangle \rightarrow |\sigma(k)+1\rangle$ and has pulse area $\pi/d_{\sigma(k)}$. This decomposition is optimal in the sense that a complete inversion of the ensemble populations cannot be achieved with $K' < K$ control pulses if the initial populations w_n satisfy $w_n \neq w_m$ for $n \neq m$.

As an example, we again apply the scheme to the N -level Morse oscillator with energy levels (2) and transition dipole moments (3) described above. To be specific, we assume that the system is initially in thermal equilibrium at a temperature $(E_4 - E_1)/k$, i.e., the initial populations of the energy eigenstates are given by the Boltzmann distribution

$$w_n = \frac{\exp[(E_n - E_1)/(E_N - E_1)]}{\sum_{k=1}^N \exp[(E_k - E_1)/(E_N - E_1)]} \quad (45)$$

for $n = 1, 2, 3, 4$. Note that the initial populations satisfy $w_1 < w_2 < w_3 < w_4$. Our goal is to create an anti-thermal ensemble, i.e., an ensemble where the populations of the energy eigenstates are reversed so that the ground state $|1\rangle$ has the lowest population w_4 , and the highest excited state has the highest population w_1 , etc. Figure 5 shows the result of control simulations using square-wave and Gaussian controls, respectively. Note that each pulse in the control sequence interchanges the populations of two adjacent energy levels until a complete reversal of the populations is achieved; for our four-level system with initial populations w_n the effect of the controls on the populations can be summarized as follows

$$\begin{array}{l} f_1 \quad f_2 \quad f_3 \quad f_1 \quad f_2 \quad f_1 \\ |1\rangle : w_1 \rightarrow w_2 \rightarrow w_2 \rightarrow w_2 \rightarrow w_3 \rightarrow w_3 \rightarrow w_4 \\ |2\rangle : w_2 \rightarrow w_1 \rightarrow w_3 \rightarrow w_3 \rightarrow w_2 \rightarrow w_4 \rightarrow w_3 \\ |3\rangle : w_3 \rightarrow w_3 \rightarrow w_1 \rightarrow w_4 \rightarrow w_4 \rightarrow w_2 \rightarrow w_2 \\ |4\rangle : w_4 \rightarrow w_4 \rightarrow w_4 \rightarrow w_1 \rightarrow w_1 \rightarrow w_1 \rightarrow w_1 \end{array}$$

where f_m refers to a control pulse of frequency μ_m and pulse area π/d_m for $m = 1, 2, 3$. The first pulse interchanges the populations of levels $|1\rangle$ and $|2\rangle$, the second pulse flips the populations of levels $|2\rangle$ and $|3\rangle$, the third pulse switches the populations of levels $|3\rangle$ and $|4\rangle$, etc.

Also note that the energy of the system increases monotonically from its minimum value in thermal equilibrium to its kinematical maximum value at the final time, as expected, where the gradient of approach is more uniform for square-wave pulses than for Gaussian wavepackets. As regards off-resonant effects, the same considerations as in the previous section apply, since $C_k = \pi/2$ for all pulses, as in the previous example.

VII. CREATION OF ARBITRARY SUPERPOSITION STATES

In this section we consider the problem of creating arbitrary superposition states from an initial state. Control schemes that create such superposition states may prove very useful in controlling quantum interference in multi-state systems and can be considered a generalization of $\pi/2$ pulses used routinely in free induction-decay experiments. To be specific, we assume that the system is initially in the ground state $|1\rangle$ and that the goal is to achieve a superposition state $|\Psi(t)\rangle$. Observe that any (normalized) superposition state can be conveniently written as

$$|\Psi(t)\rangle = \sum_{n=1}^N r_n e^{i\theta_n} |\tilde{n}(t)\rangle, \quad (46)$$

where $|\tilde{n}(t)\rangle = e^{-iE_n t} |n\rangle$ is a rotating frame and the coefficients r_n satisfy the normalization condition $\sum_{n=1}^N r_n^2 = 1$. Thus, in order to reach the target state $|\Psi(t)\rangle$ at time T we need to find a unitary operator $\hat{U}(T)$ such that

$$\hat{U}(T) \begin{pmatrix} 1 \\ 0 \\ \vdots \\ 0 \end{pmatrix} = \begin{pmatrix} r_1 e^{i(\theta_1 - E_1 T)} \\ r_2 e^{i(\theta_2 - E_2 T)} \\ \vdots \\ r_N e^{i(\theta_N - E_N T)} \end{pmatrix}. \quad (47)$$

However, note that it actually suffices to find a unitary operator \hat{U}_1 such that

$$\hat{U}_1 \begin{pmatrix} 1 \\ 0 \\ \vdots \\ 0 \end{pmatrix} = \begin{pmatrix} r_1 \\ r_2 \\ \vdots \\ r_N \end{pmatrix} \quad (48)$$

since if \hat{U}_1 satisfies (48) then $\hat{U}(T) = \hat{\Theta}(T)\hat{U}_1$ where

$$\hat{\Theta}(T) \equiv \text{diag}(e^{i(\theta_1 - E_1 T)}, \dots, e^{i(\theta_N - E_N T)}) \quad (49)$$

automatically satisfies (47). In order to find a unitary operator \hat{U}_1 that satisfies (48) we set

$$\hat{U}^{(0)} = \left(\begin{array}{c|c} r_1 & \mathbf{0} \\ \hline r_2 & \\ \vdots & \hat{I}_{N-1} \\ r_N & \end{array} \right), \quad (50)$$

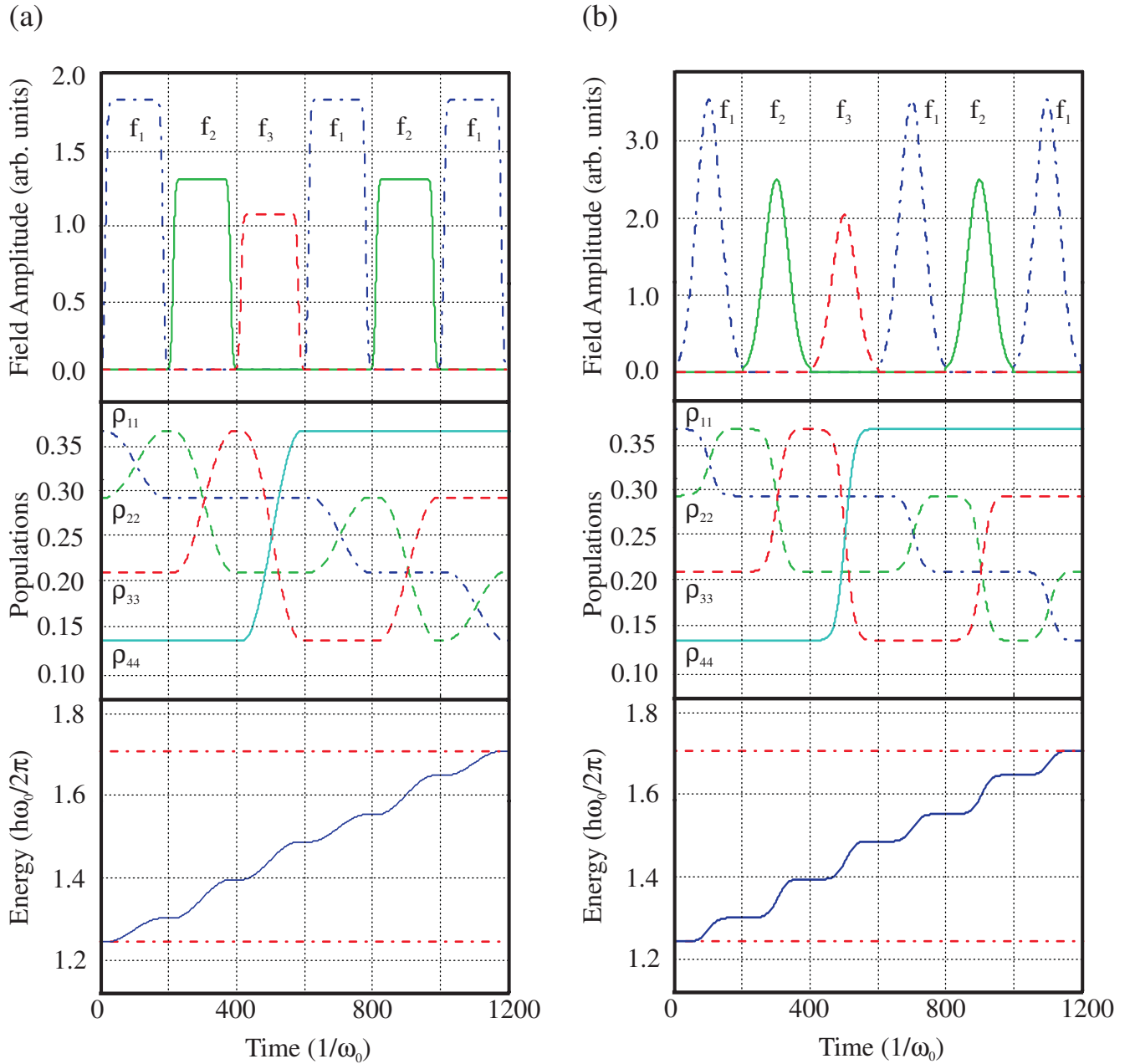


FIG. 5: Population inversion for a four-level Morse oscillator initially in thermal equilibrium using six square-wave control pulses with rise and decay time $\tau_0 = 30$ time units (a) and Gaussian pulses with shape factor $q = 4/100$ (b). Each pulse labeled f_m is resonant with the transition $|m\rangle \rightarrow |m+1\rangle$ and has pulse area π/d_m .

where \hat{I}_{N-1} is the identity matrix in dimension $N-1$, and perform Gram-Schmidt orthonormalization on the columns of $\hat{U}^{(0)}$. The resulting matrix \hat{U}_1 will be unitary and satisfy (48). To determine the control pulse sequence, we then apply the decomposition algorithm presented in appendix B to factor the target operator

$$\hat{U} = \hat{U}_0(T)^\dagger \hat{\Theta}(T) \hat{U}_1 = \Theta(0) \hat{U}_1. \quad (51)$$

As an example, let us consider the problem of creating

the superposition state

$$|\Psi(t)\rangle = \frac{1}{2} \sum_{n=1}^4 |\tilde{n}(t)\rangle = \frac{1}{2} \sum_{n=1}^4 e^{-iE_n t} |n\rangle \quad (52)$$

for a four-level system initially in state $|1\rangle$. In order to

find a unitary operator \hat{U} such that

$$\hat{U} \begin{pmatrix} 1 \\ 0 \\ 0 \\ 0 \end{pmatrix} = \begin{pmatrix} 1/2 \\ 1/2 \\ 1/2 \\ 1/2 \end{pmatrix} \quad (53)$$

we set

$$\hat{U}^{(0)} = \begin{pmatrix} 1/2 & 0 & 0 & 0 \\ 1/2 & 1 & 0 & 0 \\ 1/2 & 0 & 1 & 0 \\ 1/2 & 0 & 0 & 1 \end{pmatrix}. \quad (54)$$

and perform Gram-Schmidt orthonormalization on the columns of $\hat{U}^{(0)}$, which gives

$$\hat{U}_1 = \begin{pmatrix} 1/2 & -\sqrt{3}/6 & -\sqrt{6}/6 & -\sqrt{2}/2 \\ 1/2 & +\sqrt{3}/2 & 0 & 0 \\ 1/2 & -\sqrt{3}/6 & +\sqrt{6}/3 & 0 \\ 1/2 & -\sqrt{3}/6 & -\sqrt{6}/6 & +\sqrt{2}/2 \end{pmatrix}. \quad (55)$$

Since $\hat{\Theta}(T) = \hat{U}_0(T)$, the target operator is simply $\hat{U}_0(T)^\dagger \hat{\Theta}(T) \tilde{U} = \hat{U}_1$. Applying the decomposition algorithm described in appendix B leads to the following factorization of \hat{U}_1 :

$$\hat{U}_1 = \hat{V}_5 \hat{V}_4 \hat{V}_3 \hat{V}_2 \hat{V}_1, \quad (56)$$

where the factors are

$$\begin{aligned} \hat{V}_1 &= \exp(+C_1 \hat{x}_1), & C_1 &= \frac{\pi}{3}, \\ \hat{V}_2 &= \exp(-C_2 \hat{x}_2), & C_2 &= \arctan(\sqrt{2}) \\ \hat{V}_3 &= \exp(+C_3 \hat{x}_3), & C_3 &= \frac{\pi}{4}, \\ \hat{V}_4 &= \exp(+C_4 \hat{x}_2), & C_4 &= \frac{\pi}{2}, \\ \hat{V}_5 &= \exp(-C_5 \hat{x}_1), & C_5 &= \frac{\pi}{2}. \end{aligned} \quad (57)$$

This decomposition corresponds to the following sequence of five control pulses

$$\begin{aligned} f_1(t) &= A_1(t) e^{i(\mu_1 t + \pi/2)} + \text{c.c.} = -2A_1(t) \sin(\mu_1 t) \\ f_2(t) &= A_2(t) e^{i(\mu_2 t - \pi/2)} + \text{c.c.} = +2A_2(t) \sin(\mu_2 t) \\ f_3(t) &= A_3(t) e^{i(\mu_3 t + \pi/2)} + \text{c.c.} = -2A_3(t) \sin(\mu_3 t) \\ f_4(t) &= A_4(t) e^{i(\mu_2 t + \pi/2)} + \text{c.c.} = -2A_4(t) \sin(\mu_2 t) \\ f_5(t) &= A_5(t) e^{i(\mu_1 t - \pi/2)} + \text{c.c.} = +2A_5(t) \sin(\mu_1 t) \end{aligned}$$

with pulse areas $2\pi/3d_1$, $2 \arctan(\sqrt{2})/d_2$, $\pi/2d_3$, π/d_2 and π/d_1 , respectively. Note that only five instead of six pulses are required in this case since the target operator \hat{U}_1 has two consecutive zeros in the last column, which implies that one of the six control pulses has zero amplitude and can thus be omitted. The results of two control simulations based on this decomposition of \hat{U}_1 using square-wave and Gaussian control pulses, respectively, are presented in figure 6. Observe that the expectation value of the projector onto the target state $|\Psi(t)\rangle$ assumes its upper bound of one at the final time in both

cases, which implies that the system has indeed reached the target state $|\Psi(t)\rangle$.

Unlike decompositions (41) and (44) in the previous sections, in which the initial phases ϕ_m of the control pulses were arbitrary, the factorization (56) fixes the pulse area and frequency μ_m as well as the initial phase ϕ_m of each pulse. While the dependence of the control scheme on the pulse area and frequency is expected, the dependence on the initial phases of pulses may be a reason for concern. Thus, the question arises how the initial phases of the control pulses affect the outcome of the control process. In order to answer this question, we compute the unitary operator

$$\hat{U}_2 = \tilde{V}_5 \tilde{V}_4 \tilde{V}_3 \tilde{V}_2 \tilde{V}_1, \quad (58)$$

where the factors are

$$\begin{aligned} \tilde{V}_1 &= \exp [C_1 (\sin \phi_1 \hat{x}_1 - \cos \phi_1 \hat{y}_1)], \\ \tilde{V}_2 &= \exp [C_2 (\sin \phi_2 \hat{x}_2 - \cos \phi_2 \hat{y}_2)], \\ \tilde{V}_3 &= \exp [C_3 (\sin \phi_3 \hat{x}_3 - \cos \phi_3 \hat{y}_3)], \\ \tilde{V}_4 &= \exp [C_4 (\sin \phi_4 \hat{x}_2 - \cos \phi_4 \hat{y}_2)], \\ \tilde{V}_5 &= \exp [C_5 (\sin \phi_5 \hat{x}_1 - \cos \phi_5 \hat{y}_1)] \end{aligned} \quad (59)$$

and the constants C_k are as in (57) but the initial phases ϕ_k of the control pulses are allowed to be arbitrary, and apply this operator to the initial state $|1\rangle$. The resulting state

$$\hat{U}_2 \begin{pmatrix} 1 \\ 0 \\ 0 \\ 0 \end{pmatrix} = \begin{pmatrix} 1/2 e^{i(\phi_4 + \phi_5 - \phi_1 - \phi_2)} \\ 1/2 e^{i(-\pi/2 - \phi_5)} \\ 1/2 e^{i(\pi - \phi_1 - \phi_4)} \\ 1/2 e^{i(\pi/2 - \phi_1 - \phi_2 - \phi_3)} \end{pmatrix}. \quad (60)$$

differs from the desired target state only in the phase factors, i.e., the pulse phases do not affect the relative amplitudes r_n of the superposition state created. Furthermore, we can make the phase factors equal one by choosing $\phi_2 = \pi/2 - 2\phi_1$, $\phi_3 = \phi_1$, $\phi_4 = \pi - \phi_1$ and $\phi_5 = -\pi/2$, where ϕ_1 can be arbitrary. Note that the choice $\phi_1 = \pi/2$, $\phi_2 = -\pi/2$, $\phi_3 = \pi/2$, $\phi_4 = \pi/2$ and $\phi_5 = -\pi/2$ we made above satisfies these conditions. Recalling that we expanded the state with respect to a rotating frame $|\tilde{n}(t)\rangle = e^{-iE_n t} |n\rangle$, shows that the phases associated with the energy eigenstates in this superposition state are oscillating rapidly compared to the length of the control pulses. It is therefore hardly surprising that control of relative phases between the energy eigenstates in the superposition state requires control over the pulse phases.

VIII. OPTIMIZATION OF OBSERVABLES

Finally, we address the problem of maximizing the ensemble average of an arbitrary observable for a system whose initial state is an ensemble of energy eigenstates (26). Let us first consider the case of a time-independent

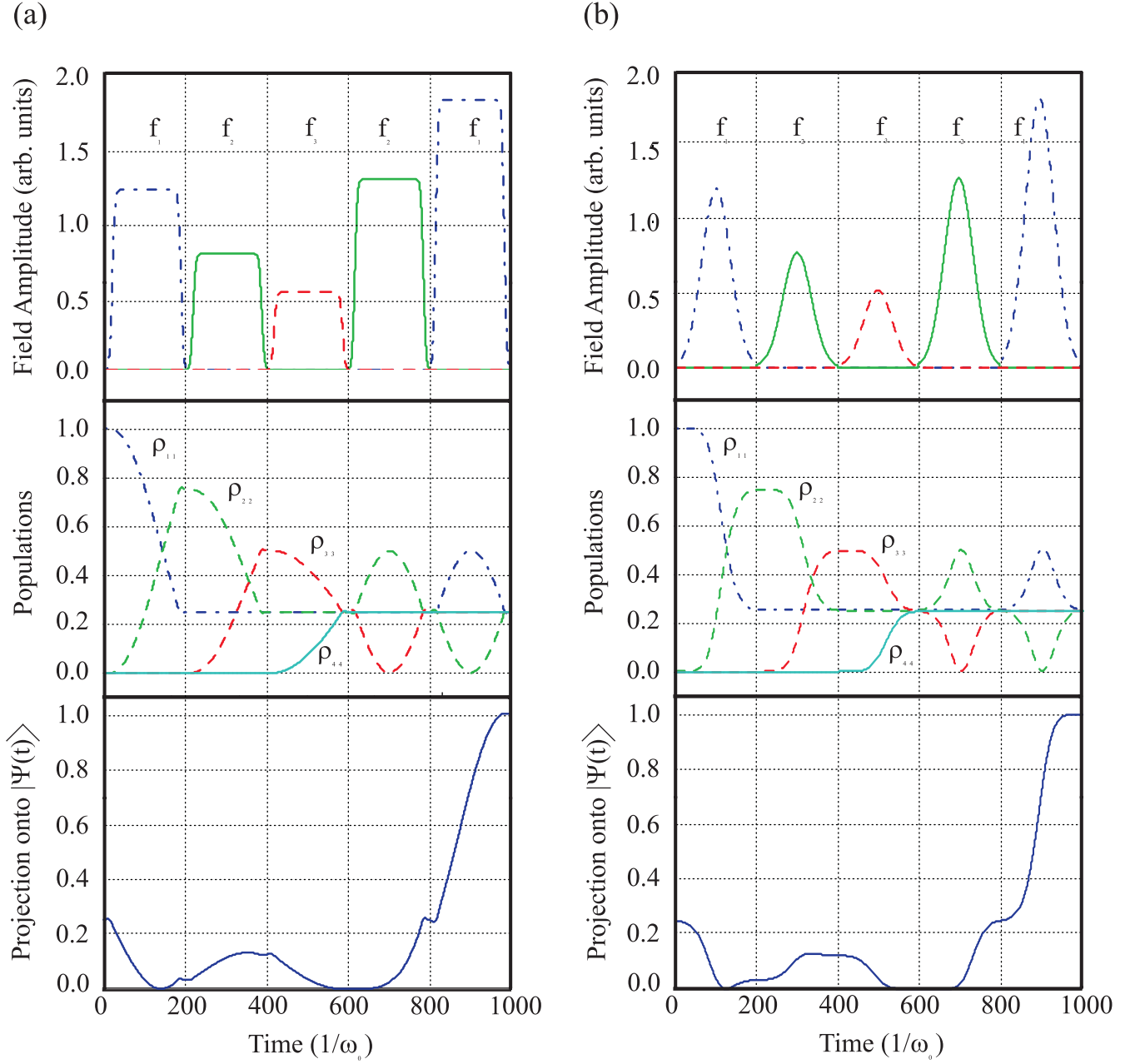


FIG. 6: Creation of the superposition state $|\Psi(t)\rangle = \frac{1}{2} \sum_{n=1}^4 |\tilde{n}(t)\rangle$ for a four-level Morse oscillator initially in the ground state $|1\rangle$ using square-wave control pulses with rise and decay time $\tau_0 = 30$ time units (a) and Gaussian control pulses with shape factor $q = 4/100$ (b). Each pulse labeled f_m is resonant with the transition $|m\rangle \rightarrow |m+1\rangle$. The pulse areas are $2\pi/3d_1$, $2\arctan(\sqrt{2})/d_2$, $\pi/2d_3$, π/d_2 and π/d_1 , respectively.

observable \hat{A} . To determine the target operator required to maximize the ensemble average $\langle \hat{A} \rangle$ of \hat{A} we observe that $\langle \hat{A} \rangle$ is bounded above by the kinematical upper bound [18]

$$\langle \hat{A} \rangle \leq \sum_{n=1}^N w_{\sigma(n)} \lambda_n, \quad (61)$$

where λ_n are the eigenvalues of \hat{A} counted with multiplicity and ordered in a non-increasing sequence

$$\lambda_1 \geq \lambda_2 \geq \dots \geq \lambda_N, \quad (62)$$

and w_n are the populations of the energy levels E_n of the initial ensemble and σ is a permutation of $\{1, \dots, N\}$ such that

$$w_{\sigma(1)} \geq w_{\sigma(2)} \geq \dots \geq w_{\sigma(N)}. \quad (63)$$

Observe that this universal upper bound for the ensemble average of any observable \hat{A} is dynamically attainable since the systems considered in this paper are completely controllable [19, 20].

Let $|\Psi_n\rangle$ for $1 \leq n \leq N$ denote the normalized eigenstates of \hat{A} satisfying $\hat{A}|\Psi_n\rangle = \lambda_n|\Psi_n\rangle$ and let \hat{U}_1 be a unitary transformation such that

$$|\Psi_{\sigma(n)}\rangle = \hat{U}_1|n\rangle, \quad 1 \leq n \leq N. \quad (64)$$

Given an initial state $\hat{\rho}_0$ of the form (26), we have

$$\begin{aligned} \text{Tr} \left(\hat{A} \hat{U}_1 \hat{\rho}_0 \hat{U}_1^\dagger \right) &= \text{Tr} \left(\hat{A} \sum_n w_n \hat{U}_1 |n\rangle \langle n| \hat{U}_1^\dagger \right) \\ &= \text{Tr} \left(\sum_n w_n \hat{A} |\Psi_{\sigma(n)}\rangle \langle \Psi_{\sigma(n)}| \right) \\ &= \text{Tr} \left(\sum_n w_n \lambda_{\sigma(n)} |\Psi_{\sigma(n)}\rangle \langle \Psi_{\sigma(n)}| \right) \\ &= \sum_n w_n \lambda_{\sigma(n)} = \sum_n w_{\sigma(n)} \lambda_n. \end{aligned} \quad (65)$$

Hence, if the system is initially in the state (26) then \hat{U}_1 is a target operator for which the observable \hat{A} assumes its kinematical maximum and we can use the decomposition algorithm described in appendix B to obtain the required factorization of the operator $\hat{U}_I = \hat{U}_0(T)^\dagger \hat{U}_1$.

However, if \hat{A} is an observable whose eigenstates are not energy eigenstates, then the expectation value or ensemble average of \hat{A} will usually oscillate rapidly as a result of the action of the free evolution operator $\hat{U}_0(t)$. These oscillations are rarely significant for the application at hand and often distracting. In such cases it is advantageous to define a dynamic observable

$$\tilde{A}(t) = \hat{U}_0(t) \hat{A} \hat{U}_0(t)^\dagger \quad (66)$$

and optimize its ensemble average instead. To accomplish this, note that if $|\Psi_n\rangle$ are the eigenstates of \hat{A} satisfying $\hat{A}|\Psi_n\rangle = \lambda_n|\Psi_n\rangle$ then $|\tilde{\Psi}_n(t)\rangle = \hat{U}(t)|\Psi_n\rangle$ are the corresponding eigenstates of $\tilde{A}(t)$ since

$$\begin{aligned} \tilde{A}(t)|\tilde{\Psi}_n(t)\rangle &= \hat{U}(t) \hat{A} \hat{U}(t)^\dagger \hat{U}(t)|\Psi_n\rangle \\ &= \hat{U}(t) \lambda_n |\Psi_n\rangle \\ &= \lambda_n |\tilde{\Psi}_n(t)\rangle \end{aligned}$$

and if \hat{U}_1 is a unitary operator such that equation (64) holds then $\hat{U}_0(t) \hat{U}_1$ is a unitary operator that maps the energy eigenstates $|n\rangle$ onto the $\tilde{A}(t)$ -eigenstates $|\tilde{\Psi}_n(t)\rangle$ since

$$\hat{U}_0(t) \hat{U}_1 |n\rangle = \hat{U}_0(t) |\Psi_{\sigma(n)}\rangle = |\tilde{\Psi}_{\sigma(n)}(t)\rangle$$

for $1 \leq n \leq N$. Thus, the evolution operator required to maximize the ensemble average of $\tilde{A}(t)$ at time $T > 0$

is $\hat{U}_0(T) \hat{U}_1$ and the target operator to be decomposed as described in appendix B is

$$\hat{U} = \hat{U}_0(T)^\dagger \hat{U}_0(T) \hat{U}_1 = \hat{U}_1. \quad (67)$$

For instance, suppose we wish to maximize the ensemble average of the transition dipole moment operator $\hat{A}(t) = \hat{U}_0(t) \hat{A} \hat{U}_0(t)^\dagger$, where

$$\hat{A} = \sum_{n=1}^{N-1} d_n (|n\rangle \langle n+1| + |n+1\rangle \langle n|), \quad (68)$$

for a system initially in state (26) with

$$w_1 > w_2 > \dots > w_N > 0. \quad (69)$$

Then we need to find a unitary operator \hat{U}_1 that maps the initial state $|n\rangle$ onto the \hat{A} -eigenstate $|\Psi_n\rangle$ for $1 \leq n \leq N$. To accomplish this we let \hat{U}_1 be the $N \times N$ matrix whose n th column is the normalized \hat{A} -eigenstate $|\Psi_n\rangle$. Then \hat{U}_1 clearly satisfies $\hat{U}_1|n\rangle = |\Psi_n\rangle$ and since $\langle \Psi_n | \Psi_m \rangle = \delta_{n,m}$ by hypothesis, i.e., the eigenstates are orthonormal, \hat{U}_1 is automatically unitary.

For $N = 4$ and $d_n = \sqrt{n}$ the eigenvalues of the operator \hat{A} defined in equation (68) are (in decreasing order)

$$\lambda_1 = \sqrt{3 + \sqrt{6}}, \quad \lambda_2 = \sqrt{3 - \sqrt{6}}, \quad \lambda_3 = -\lambda_2, \quad \lambda_4 = -\lambda_1$$

and the corresponding eigenstates with respect to the standard basis $|n\rangle$ are the columns of the operator

$$\hat{U}_1 = \begin{bmatrix} \frac{1}{2\lambda_1} & \frac{1}{2\lambda_2} & \frac{1}{2\lambda_2} & \frac{1}{2\lambda_1} \\ \frac{1}{2} & \frac{1}{2} & -\frac{1}{2} & -\frac{1}{2} \\ \frac{\sqrt{2}+\sqrt{3}}{2\lambda_1} & \frac{\sqrt{2}-\sqrt{3}}{2\lambda_2} & \frac{\sqrt{2}-\sqrt{3}}{2\lambda_2} & \frac{\sqrt{2}+\sqrt{3}}{2\lambda_1} \\ \frac{1}{2} & -\frac{1}{2} & \frac{1}{2} & -\frac{1}{2} \end{bmatrix}. \quad (70)$$

Applying the decomposition algorithm described in appendix B yields the following factorization

$$\hat{U}_1 \hat{\Theta} = \hat{V}_6 \hat{V}_5 \hat{V}_4 \hat{V}_3 \hat{V}_2 \hat{V}_1, \quad (71)$$

where the factors are

$$\begin{aligned} \hat{V}_1 &= \exp(-C_1 \hat{x}_1), \quad C_1 = \pi/4, \\ \hat{V}_2 &= \exp(-C_2 \hat{x}_2), \quad C_2 = \arctan(\sqrt{2}), \\ \hat{V}_3 &= \exp(-C_3 \hat{x}_1), \quad C_3 = \text{arccot}\left(\frac{\sqrt{6}-\sqrt{3}+3\sqrt{2}}{3}\right), \\ \hat{V}_4 &= \exp(-C_4 \hat{x}_3), \quad C_4 = \pi/3, \\ \hat{V}_5 &= \exp(-C_5 \hat{x}_2), \quad C_5 = \arctan\left(\frac{\sqrt{4+\sqrt{6}}}{\sqrt{2+\sqrt{3}}}\right), \\ \hat{V}_6 &= \exp(-C_6 \hat{x}_1), \quad C_6 = \text{arccot}\left(\sqrt{3+\sqrt{6}}\right) \end{aligned} \quad (72)$$

and $\hat{\Theta} = \text{diag}(1, -1, 1, -1)$. Note that $\hat{U}_2 \equiv \hat{U}_1 \hat{\Theta}$ is equivalent to \hat{U}_1 since $\hat{\Theta}$ commutes with $\hat{\rho}_0$ as defined in equation (26), i.e., $\hat{\Theta} \hat{\rho}_0 \hat{\Theta}^\dagger = \hat{\rho}_0$, and thus

$$\begin{aligned} \text{Tr} \left(\hat{A} \hat{U}_2 \hat{\rho}_0 \hat{U}_2^\dagger \right) &= \text{Tr} \left(\hat{A} \hat{U}_1 \hat{\Theta} \hat{\rho}_0 \hat{\Theta}^\dagger \hat{U}_1^\dagger \right) \\ &= \text{Tr} \left(\hat{A} \hat{U}_1 \hat{\rho}_0 \hat{U}_1 \right). \end{aligned} \quad (73)$$

Decomposition (71) corresponds to the following sequence of six control pulses

$$\begin{aligned}
f_1(t) &= A_1(t)e^{i(\mu_1 t - \pi/2)} + \text{c.c.} = 2A_1(t) \sin(\mu_1 t) \\
f_2(t) &= A_2(t)e^{i(\mu_2 t - \pi/2)} + \text{c.c.} = 2A_2(t) \sin(\mu_2 t) \\
f_3(t) &= A_3(t)e^{i(\mu_1 t - \pi/2)} + \text{c.c.} = 2A_3(t) \sin(\mu_1 t) \\
f_4(t) &= A_4(t)e^{i(\mu_3 t - \pi/2)} + \text{c.c.} = 2A_4(t) \sin(\mu_3 t) \\
f_5(t) &= A_5(t)e^{i(\mu_2 t - \pi/2)} + \text{c.c.} = 2A_5(t) \sin(\mu_2 t) \\
f_6(t) &= A_6(t)e^{i(\mu_1 t - \pi/2)} + \text{c.c.} = 2A_6(t) \sin(\mu_1 t)
\end{aligned}$$

with pulse areas $\pi/2d_1$, $2C_2/d_2$, $2C_3/d_1$, $2\pi/3d_3$, $2C_5/d_2$, $2C_6/d_1$, respectively. Again, the decomposition fixes the frequency and pulse area as well as the initial phase of each pulse, and the question thus arises, what role the phases play. As we have already seen above, the target operator \hat{U}_1 is not unique. In fact, equation (73) shows that right multiplication of \hat{U}_1 by any unitary matrix that commutes with $\hat{\rho}_0$ produces another unitary operator that is equivalent to \hat{U}_1 in that both evolution operators lead to the same ensemble average of the target observable. Nevertheless, in general, the control process is sensitive to the phases ϕ_m . For instance, one can verify that changing the phase ϕ_1 of the first pulse from $-\pi/2$ to $\pi/2$ in the pulse sequence above leads to the following evolution operator

$$\hat{U}_3 = \begin{bmatrix} \frac{1}{2\lambda_2} & \frac{1}{2\lambda_1} & \frac{1}{2\lambda_2} & -\frac{1}{2\lambda_1} \\ \frac{1}{2} & \frac{1}{2} & -\frac{1}{2} & \frac{1}{2} \\ \frac{\sqrt{2}-\sqrt{3}}{2\lambda_2} & \frac{\sqrt{2}+\sqrt{3}}{2\lambda_1} & \frac{\sqrt{2}-\sqrt{3}}{2\lambda_2} & \frac{\sqrt{2}+\sqrt{3}}{-2\lambda_1} \\ -\frac{1}{2} & \frac{1}{2} & \frac{1}{2} & \frac{1}{2} \end{bmatrix}, \quad (74)$$

which maps $|3\rangle$ onto $|\Psi_3\rangle$ and $|4\rangle$ onto $-|\Psi_4\rangle$ but $|1\rangle$ onto $|\Psi_2\rangle$ and $|2\rangle$ onto $|\Psi_1\rangle$ and thus leads to the ensemble average

$$\langle \hat{A} \rangle = w_1 \lambda_2 + w_2 \lambda_1 + w_3 \lambda_3 + w_4 \lambda_4 \quad (75)$$

at the final time, which is strictly less than the kinematical maximum if $w_1 > w_2$.

Figure 7 shows the results of control simulations based on the control pulse sequence above for our four-level Morse oscillator initially in thermal equilibrium using square-wave and Gaussian control pulses, respectively. Observe that the observable indeed attains its kinematical upper bound at the final time, as desired.

IX. CONCLUSION

We have presented several control schemes designed to achieve a wide variety of control objectives ranging from population transfers and inversions of ensemble populations to creation of superposition states and optimization of observables. The main advantage of the schemes is their simplicity: the control objective is achieved by applying a sequence of simple control pulses such as square-wave pulses with finite rise and decay times, which can be created in the laboratory by modulating the amplitude of CW lasers using Pockel cells, or Gaussian wavepackets, which can be obtained from pulsed laser sources. The main shortcoming of this control approach is the need to be able to address a single transition at a time, which limits the applicability of this technique to systems with sufficiently distinct transition frequencies (as regards the controlled transitions) to permit frequency-selective control, unless other selection rules can be employed to address transitions individually. Another possible complication arises from unwanted off-resonant effects. However, as we have demonstrated, in general it is possible to limit such effects by using sufficiently weak control pulses.

APPENDIX A: DERIVATION OF EQUATION (16)

Inserting equations (14) and (7) into equation (15) and recalling $\mu_m = E_{m+1} - E_m$ leads to

$$\begin{aligned}
i \frac{d\hat{U}_I(t)}{dt} &= \hat{U}_0(t)^\dagger \left\{ \sum_{m=1}^M \hat{H}_m[f_m(t)] \right\} \hat{U}_0(t) \hat{U}_I(t) \\
&= \sum_{n,m,n'} e^{iE_n t} \hat{e}_{n,n} \left(A_m(t) e^{i(\mu_m t + \phi_m)} d_m \hat{e}_{m,m+1} + A_m(t) e^{-i(\mu_m t + \phi_m)} d_m \hat{e}_{m+1,m} \right) e^{-iE_{n'} t} \hat{e}_{n',n'} \hat{U}_I(t) \\
&= \sum_m \left(A_m(t) d_m e^{iE_m t} e^{i(\mu_m t + \phi_m)} e^{-iE_{m+1} t} \hat{e}_{m,m+1} + A_m(t) d_m e^{iE_{m+1} t} e^{-i(\mu_m t + \phi_m)} e^{-iE_m t} \hat{e}_{m+1,m} \right) \hat{U}_I(t) \\
&= \sum_m A_m(t) d_m \left(e^{i\phi_m} \hat{e}_{m,m+1} + e^{-i\phi_m} \hat{e}_{m+1,m} \right) \hat{U}_I(t) \\
&= \sum_m A_m(t) d_m \left[\cos \phi_m (\hat{e}_{m,m+1} + \hat{e}_{m+1,m}) + i \sin \phi_m (\hat{e}_{m,m+1} - \hat{e}_{m+1,m}) \right] \hat{U}_I(t)
\end{aligned}$$

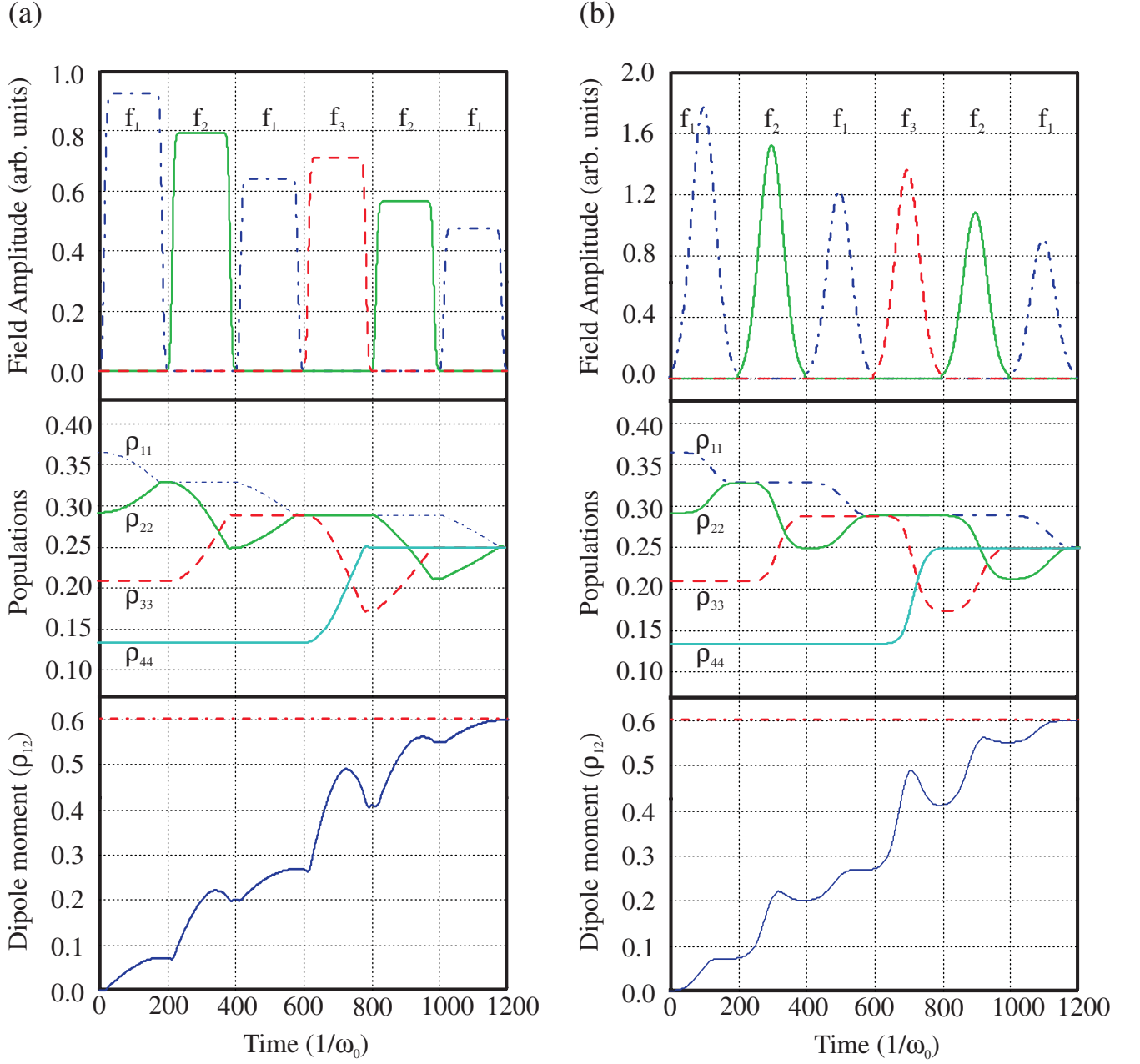


FIG. 7: Maximization of the (dynamic) transition dipole moment operator $\hat{A}(t)$ for a four-level Morse oscillator initially in thermal equilibrium using square-wave control pulses with rise and decay time $\tau_0 = 30$ time units (a) and Gaussian control pulses with shape factor $q = 4/100$ (b).

$$= \sum_m A_m(t) d_m (-i \cos \phi_m \hat{y}_m + i \sin \phi_m \hat{x}_m) \hat{U}_I(t).$$

Hence, multiplying both sides by $-i$ gives

$$\frac{d\hat{U}_I(t)}{dt} = \sum_m A_m(t) d_m (\sin \phi_m \hat{x}_m - \cos \phi_m \hat{y}_m) \hat{U}_I(t). \quad (\text{A1})$$

APPENDIX B: LIE GROUP DECOMPOSITION ALGORITHM

To find a decomposition of the form (23) for a given unitary operator \hat{U} , we set

$$\hat{U}^{(0)} \equiv e^{-i\Gamma/N} \hat{U}, \quad (\text{B1})$$

where $e^{i\Gamma} \equiv \det(\hat{U})$, to ensure that $\hat{U}^{(0)} \in SU(N)$. Our goal is to reduce this matrix $\hat{U}^{(0)}$ step by step to a diagonal matrix whose diagonal elements are arbitrary phase factors $e^{i\theta_n}$. Recall that this reduction is always sufficient if the initial state of the system is an ensemble of energy eigenstates.

Let $U_{ij}^{(0)}$ denote the i th row and j th column entry in the matrix representation of $\hat{U}^{(0)}$. In the first step of the decomposition we wish to find a matrix

$$\hat{W}^{(1)} = \exp[-C_1 (\sin \phi_1 \hat{x}_1 - \cos \phi_1 \hat{y}_1)], \quad (\text{B2})$$

which is the identity matrix everywhere except for a 2×2 block of the form

$$\begin{pmatrix} \cos(C_1) & ie^{i\phi_1} \sin(C_1) \\ ie^{-i\phi_1} \sin(C_1) & \cos(C_1) \end{pmatrix} \quad (\text{B3})$$

in the top left corner, such that

$$\hat{W}^{(1)} \begin{pmatrix} U_{1,N}^{(0)} \\ U_{2,N}^{(0)} \\ \vdots \\ \vdots \end{pmatrix} = \begin{pmatrix} 0 \\ c \\ \vdots \\ \vdots \end{pmatrix} \quad (\text{B4})$$

where c is some complex number. Noting that

$$U_{1,N}^{(0)} = r_1 e^{i\alpha_1}, \quad U_{2,N}^{(0)} = r_2 e^{i\alpha_2}$$

it can easily be verified that setting

$$\begin{aligned} \phi_k &= \pi/2 + \alpha_1 - \alpha_2 \\ C_k &= -\text{arccot}(-r_2/r_1) \end{aligned} \quad (\text{B5})$$

achieves (B4). Next we set

$$\hat{U}^{(1)} = \hat{W}^{(1)} \hat{U}^{(0)} \quad (\text{B6})$$

and find $\hat{W}^{(2)}$ of the form

$$\hat{W}^{(2)} = \exp[-C_2 (\sin \phi_2 \hat{x}_2 - \cos \phi_2 \hat{y}_2)] \quad (\text{B7})$$

such that

$$\hat{W}^{(2)} \begin{pmatrix} 0 \\ U_{2,N}^{(1)} \\ U_{3,N}^{(1)} \\ \vdots \\ \vdots \end{pmatrix} = \begin{pmatrix} 0 \\ 0 \\ c \\ \vdots \\ \vdots \end{pmatrix} \quad (\text{B8})$$

where c is again some complex number. Repeating this procedure $N - 1$ times leads to a matrix $\hat{U}^{(N-1)}$ whose

last column is $(0, \dots, 0, e^{i\theta_N})^T$. Since we are not concerned about the phase factor $e^{i\theta_N}$ in this paper, we stop here. Noting that

$$\exp\left[-\frac{\pi}{2} \hat{x}_{N-1}\right] \times \exp\left[-\frac{\pi}{2} (\sin \phi \hat{x}_{N-1} - \cos \phi \hat{y}_{N-1})\right]$$

with $\phi = -\pi/2 - \theta_n$ maps $(0, e^{i\theta_{N-1}})^T$ onto $(0, 1)^T$, we see that complete reduction to the identity matrix would require two additional steps at this point to eliminate the phase factor $e^{i\theta_N}$, which would result in two additional control pulses.

Having reduced the last column, we continue with the $(N - 1)$ st column in the same fashion, noting that (since $\hat{U}^{(0)}$ is unitary) at most $N - 2$ steps will be required to reduce the $(N - 1)$ st column to $(0, \dots, 0, e^{i\theta_{N-1}}, 0)^T$. We repeat this procedure until after (at most) $K = N(N - 1)/2$ steps $\hat{U}^{(0)}$ is reduced to a diagonal matrix $\text{diag}(e^{i\theta_1}, \dots, e^{i\theta_N})$, as required and we have

$$\hat{W}^{(K)} \dots \hat{W}^{(1)} \hat{U}^{(0)} = \text{diag}(e^{i\theta_1}, \dots, e^{i\theta_N}). \quad (\text{B9})$$

Finally, setting

$$\hat{V}_k \equiv \left(\hat{W}^{(K+1-k)}\right)^\dagger \quad (\text{B10})$$

leads to

$$\hat{U}^{(0)} = \hat{V}_K \hat{V}_{K-1} \dots \hat{V}_1 \text{diag}(e^{i\theta_1}, \dots, e^{i\theta_N}) \quad (\text{B11})$$

and therefore

$$\hat{U} = \hat{V}_K \hat{V}_{K-1} \dots \hat{V}_1 \Theta, \quad (\text{B12})$$

where Θ is a diagonal matrix

$$\Theta = e^{i\Gamma/N} \text{diag}(e^{i\theta_1}, \dots, e^{i\theta_N}). \quad (\text{B13})$$

Note that \hat{U} can always be decomposed such that Θ is the identity matrix. However, to achieve this goal up to $2(N - 1)$ additional terms would be required to eliminate the phase factors, which would result in additional control pulses. While some applications may indeed require the elimination of these phase factors, the phase factors are often insignificant and the additional control pulses would be superfluous. For a more sophisticated decomposition algorithm that requires only very few phases the reader is referred to [21].

ACKNOWLEDGEMENTS

We sincerely thank A. I. Solomon and A. V. Durrant of the Open University for helpful discussions and suggestions. ADG would like to thank the EPSRC for financial support and VR would like to acknowledge the support of NSF Grant DMS 0072415.

-
- [1] H. Rabitz, R. de Vivie-Riedle, M. Motzkus, and K. Kompa, *Science* **288**, 824 (2000).
- [2] R. T. Sang, G. S. Summy, B. T. V. Varcoe, W. R. MacGillivray, and M. C. Standage, *Phys. Rev. A* **63**, 023408 (2001).
- [3] H. Umeda and Y. Fujimura, *J. Chem. Phys.* **113**(9), 3510 (2000).
- [4] D. J. Tannor, R. Kosloff, and A. Bartana, *Faraday Discuss.* **113**, 365 (1999).
- [5] S. G. Schirmer, *Phys. Rev. A* **63**(1), 069101 (2001).
- [6] G.-L. Long and Y. Sun, *quant-ph/0104030* (2001).
- [7] A. D. Greentree, S. G. Schirmer, and A. I. Solomon, *quant-ph/0103118* (2001).
- [8] B. K. Dey, *J. Phys. A* **33**, 4643 (2000).
- [9] S. G. Schirmer, M. D. Girardeau, and J. V. Leahy, *Phys. Rev. A* **61**, 012101 (2000).
- [10] A. C. Doherty, S. Habib, K. Jacobs, H. Mabuchi, and S. M. Tan, *Phys. Rev. A* **62**, 012105 (2000).
- [11] S. Lloyd and J. J. E. Slotine, *Phys. Rev. A* **62**, 012307 (2000).
- [12] Y. Ohtsuki, H. Kono, and Y. Fujimura, *J. Chem. Phys.* **109**, 9318 (1998), ISSN 0021-9606.
- [13] M. Q. Phan and H. Rabitz, *J. Chem. Phys.* **110**, 34 (1999).
- [14] Y. Ohtsuki, W. Zhu, and H. Rabitz, *J. Chem. Phys.* **110**, 9825 (1999).
- [15] V. Ramakrishna, R. Ober, X. Sun, O. Steuernagel, J. Botina, and H. Rabitz, *Phys. Rev. A* **61**, 032106 (2000).
- [16] S. G. Schirmer, A. D. Greentree, and A. I. Solomon, *quant-ph/0103117* (2001).
- [17] V. Buzek, M. Hillery, and F. Werner, *J. Modern Optics* **47**(2), 211 (2000).
- [18] M. D. Girardeau, S. G. Schirmer, J. V. Leahy, and R. M. Koch, *Phys. Rev. A* **58**, 2684 (1998).
- [19] S. G. Schirmer and J. V. Leahy, *Phys. Rev. A* **63**(2), 025403 (2001).
- [20] S. G. Schirmer, H. Fu, and A. I. Solomon, *Phys. Rev. A* **63**, 063410 (2001).
- [21] V. Ramakrishna, *Control of molecular systems with very few phases*, *Chem. Phys.*, to appear (2001).